Reovirus Cell Entry Requires Functional Microtubules

Bernardo A. Mainou,[a,b] Paula F. Zamora,[b,c] Alison W. Ashbrook,[b,c] Daniel C. Dorset,[d] Kwang S. Kim,[e] Terence S. Dermody[a,b,c]

Departments of Pediatrics,[a] Pathology, Microbiology, and Immunology,[c] Elizabeth B. Lamb Center for Pediatric Research,[b] and Vanderbilt Technologies for Advanced Genomics,[d] Vanderbilt University School of Medicine, Nashville, Tennessee, USA; Division of Pediatric Infectious Diseases, Johns Hopkins School of Medicine, Baltimore, Maryland, USA[e]

ABSTRACT **Mammalian reovirus binds to cell-surface glycans and junctional adhesion molecule A and enters cells by receptor-mediated endocytosis in a process dependent on β1 integrin. Within the endocytic compartment, reovirus undergoes stepwise disassembly, allowing release of the transcriptionally active viral core into the cytoplasm. To identify cellular mediators of reovirus infectivity, we screened a library of small-molecule inhibitors for the capacity to block virus-induced cytotoxicity. In this screen, reovirus-induced cell killing was dampened by several compounds known to impair microtubule dynamics. Microtubule inhibitors were assessed for blockade of various stages of the reovirus life cycle. While these drugs did not alter reovirus cell attachment or internalization, microtubule inhibitors diminished viral disassembly kinetics with a concomitant decrease in infectivity. Reovirus virions colocalize with microtubules and microtubule motor dynein 1 during cell entry, and depolymerization of microtubules results in intracellular aggregation of viral particles. These data indicate that functional microtubules are required for proper sorting of reovirus virions following internalization and point to a new drug target for pathogens that use the endocytic pathway to invade host cells.**

IMPORTANCE **Screening libraries of well-characterized drugs for antiviral activity enables the rapid characterization of host processes required for viral infectivity and provides new therapeutic applications for established pharmaceuticals. Our finding that microtubule-inhibiting drugs impair reovirus infection identifies a new cell-based antiviral target.**

Received 30 May 2013 **Accepted** 10 June 2013 **Published** 2 July 2013

Citation Mainou BA, Zamora PF, Ashbrook AW, Dorset DC, Kim KS, Dermody TS. 2013. Reovirus cell entry requires functional microtubules. mBio 4(4):e00405-13. doi:10.1128/mBio.00405-13.

Editor Anne Moscona, Weill Medical College—Cornell

Address correspondence to Terence S. Dermody, terry.dermody@vanderbilt.edu.

The interplay between viruses and host cells regulates each step of the virus-host encounter. Viral tropism is restricted by the availability of cell-surface receptors and host molecules that promote viral internalization, replication, assembly, and release. Understanding the cellular components that underlie productive viral infection can illuminate new targets for development of antiviral therapies, improve viral vector design, and enhance an understanding of cellular processes at the pathogen-host interface.

Mammalian orthoreovirus (called reoviruses here) are nonenveloped, double-stranded RNA viruses that are formed from two concentric protein shells (1). Reoviruses infect most mammalian species, and although most humans are exposed during childhood, infection seldom results in disease (1, 2). The reovirus genome can now be engineered using reverse genetics, leading to the recovery of viable viruses with targeted alterations (3). Coupled with the capacity to elicit mucosal immune responses (1, 4) and natural attenuation in humans (1), this technology provides an opportunity to develop reovirus as a vaccine vector. Moreover, reovirus is currently being tested in clinical trials for efficacy as an oncolytic agent against a variety of cancers (5).

Reovirus attaches to host cells via interactions with cell-surface glycans (6, 7) and junctional adhesion molecule A (JAM-A) (8–10). Following attachment to JAM-A, reovirus is internalized in a β1 integrin-dependent manner via receptor-mediated endocytosis (11). Following internalization, reovirus activates Src kinase (12) and traverses through early and late endosomes (13). In late endosomes, virions undergo stepwise acid-dependent proteolytic disassembly catalyzed by cysteine cathepsin proteases to form infectious subvirion particles (ISVPs). ISVPs are characterized by the loss of outer-capsid protein σ3 and cleavage of outer-capsid protein μ1. The μ1 cleavage fragments mediate endosomal membrane penetration and release of the transcriptionally active viral core into the cytoplasm (14–16). ISVPs also can be generated *in vitro* by treatment of virions with a variety of proteases (14, 16). These particles bind JAM-A to initiate infection but are thought to penetrate at or near the cell surface (8, 17, 18), bypassing a requirement for acid-dependent proteolytic disassembly (16, 18). Host factors that mediate internalization and endosomal transport of reovirus virions are not completely understood.

Microtubules are long, filamentous protein polymers composed of α-tubulin and β-tubulin heterodimers (19). These structures regulate a wide variety of cellular functions, including mitosis, maintenance of cell shape, and intracellular transport (19). Posttranslational modifications of tubulin subunits and the interaction of microtubule-associated proteins with microtubules regulate polymerization dynamics (20). Because of the essential role in cell division, microtubules are targets for several anticancer chemotherapeutic agents (20, 21). For example, paclitaxel was originally developed for use against ovarian cancer but also is used

to treat other cancers, including metastatic breast cancer (20–22). Vinca alkaloids, including vindesine sulfate, are used to treat non-small-cell lung cancer, leukemia, lymphoma, and breast cancer (20, 21, 23). Microtubule-inhibiting compounds are classified into two groups based on whether the drug stabilizes or destabilizes microtubules. Stabilizing agents, such as taxanes, enhance microtubule polymerization, whereas destabilizing agents, such as vinca alkaloids and colchicine, inhibit microtubule polymerization by directly binding to microtubule subunits (20). Microtubule motors are used for bidirectional transport of cargo (24). Minus-end motors (dyneins) transport cargo toward the cell interior, whereas plus-end motors (kinesins) move cargo toward the cell periphery (24). It is not known whether microtubules or microtubule motors are required for reovirus entry.

In this study, we identified microtubule inhibitors in a high-throughput screen of small molecules for blockade of reovirus-mediated cell death. These drugs do not impede reovirus attachment or internalization but delay the intracellular transport of incoming virions, with a concomitant decrease in viral infectivity. Diminished expression of the dynein 1 heavy chain by RNA interference (RNAi) decreases reovirus infection. These findings indicate that reovirus uses microtubules and dynein 1 to efficiently enter and infect host cells, providing a potential new therapeutic option for viruses that penetrate deep into the endocytic pathway to establish infection.

RESULTS

Identification of microtubule inhibitors using a high-throughput small-molecule screen. To identify cellular factors required for reovirus cytotoxicity, we performed a high-throughput screen using small molecules from the NIH Clinical Collection (NCC), a library that contains 446 compounds that have been used in phase I, II, and III clinical trials in humans (see Fig. S1A in the supplemental material). Small molecules in the NCC were initially developed for use against a variety of diseases, including central nervous system, cardiovascular, and gastrointestinal malignancies, as well as numerous anti-infectives. HeLa S3 cells, which undergo cell death following reovirus infection (25), were incubated with dimethyl sulfoxide (DMSO) (vehicle control), 10 μM cysteine-protease inhibitor E64-d as a positive control (26), or a 10 μM concentration of each of the compounds in the NCC, adsorbed with cytopathic reovirus strain T3SA+ (6, 27), and incubated for 48 h. Cellular ATP levels were assessed as a proxy for cell viability. *Z* scores were calculated to identify compounds that significantly diminished reovirus-induced cell death (see Table S1 in the supplemental material). Eleven compounds had *Z* scores of greater than 2.0, with *Z* scores in this group ranging from 2.758 to 8.444 (Fig. S1B). Interestingly, 5 of the 11 compounds identified are drugs that influence microtubule stability and function (20) (Fig. S1C). Microtubule-inhibiting compounds constitute <1% of the total number of small molecules in the NCC, suggesting that the large number of microtubule inhibitors identified does not reflect bias within the screen. Thus, these data suggest that functional microtubules are required for reovirus-induced cytotoxicity.

Microtubule inhibitors diminish reovirus-mediated cell death and infectivity. To verify that microtubule-inhibiting drugs block cytotoxicity induced by reovirus, HeLa S3 cells were incubated with DMSO, E64-d, or NH_4Cl as positive controls, or increasing concentrations of microtubule-inhibiting drugs for 1 h prior to reovirus adsorption. Cell viability was assessed by quantifying cellular ATP levels 48 h after adsorption (Fig. 1A). Similar to the observations made using the NCC screen, we observed a dose-dependent decrease in reovirus-mediated cytotoxicity with increasing concentrations of microtubule-inhibiting compounds, E64-d, or NH_4Cl. The observed inhibition was statistically significant at concentrations of 0.1 to 1.0 μM for all compounds tested except for flubendazole, which inhibited at concentrations of 1.0 and 10 μM. These data confirm findings obtained from the small-molecule screen and provide further evidence that microtubule function is required for reovirus-induced cell death.

To determine whether microtubule function is required for reovirus infectivity in epithelial and endothelial cells, we tested the effect of microtubule-inhibiting compounds on reovirus infection of CCL2 HeLa cells, HeLa S3 cells, and human brain microvascular endothelial cells (HBMECs). Both CCL2 and S3 HeLa cells are highly susceptible to reovirus infection and have been used in studies to understand cellular mediators of reovirus cell entry (12, 13). HBMECs are highly transfectable and provide a tractable model cell line for studies of virus replication in endothelial cells (28). Cells were treated with DMSO, E64-d, NH_4Cl, or increasing concentrations of microtubule inhibitors for 1 h prior to adsorption with reovirus T3SA+, incubated in the presence of inhibitors, and scored for infection by indirect immunofluorescence (Fig. 1B). For all cell lines tested, treatment with vindesine sulfate yielded a statistically significant decrease in infectivity. While colchicine and docetaxel also decreased infectivity in the cell types tested, the effects were not as pronounced as those observed with vindesine sulfate. Interestingly, among the compounds from the NCC, we identified three vinca alkaloid compounds, vindesine sulfate, vincristine sulfate, and vinorelbine bitartrate, that impaired reovirus-mediated cytotoxicity. These data suggest that vinca alkaloids are more potent as anti-infectives against reovirus than other microtubule-inhibiting agents. Together, these data indicate that microtubule function is required for maximal reovirus infectivity and reovirus-mediated cell killing.

Vindesine sulfate blocks reovirus replication at early times of infection. To define the temporal window in which microtubule inhibitors act to impair reovirus infection, CCL2 HeLa cells were treated with DMSO, NH_4Cl, or 1 μM vindesine sulfate for 1 h prior to reovirus adsorption or in 1-h increments up to 2 h post-adsorption. Cells were then incubated in the presence or absence of inhibitors and scored for infection by indirect immunofluorescence 20 h after adsorption (Fig. 2A). Since microtubules depolymerize at cold temperatures (29), virus was adsorbed at room temperature to prevent microtubule depolymerization while also allowing sufficient time for reovirus to attach to cells. For the remainder of the descriptions of our studies, 0 min represents the initiation of infection following adsorption at room temperature. Vindesine sulfate treatment 1 h prior to or immediately following adsorption substantially decreased reovirus infection. However, addition of vindesine sulfate 1 h or more after adsorption decreased reovirus infection much less efficiently. These data indicate that vindesine sulfate is most potent in diminishing reovirus infection during the first hour of the infectious cycle, suggesting that reovirus requires microtubule function during the interval required for viral entry and uncoating. In addition, these findings demonstrate that impairment of reovirus infection by vindesine sulfate is not attributable to toxicity of the compound.

To determine whether vindesine sulfate impairs infection by

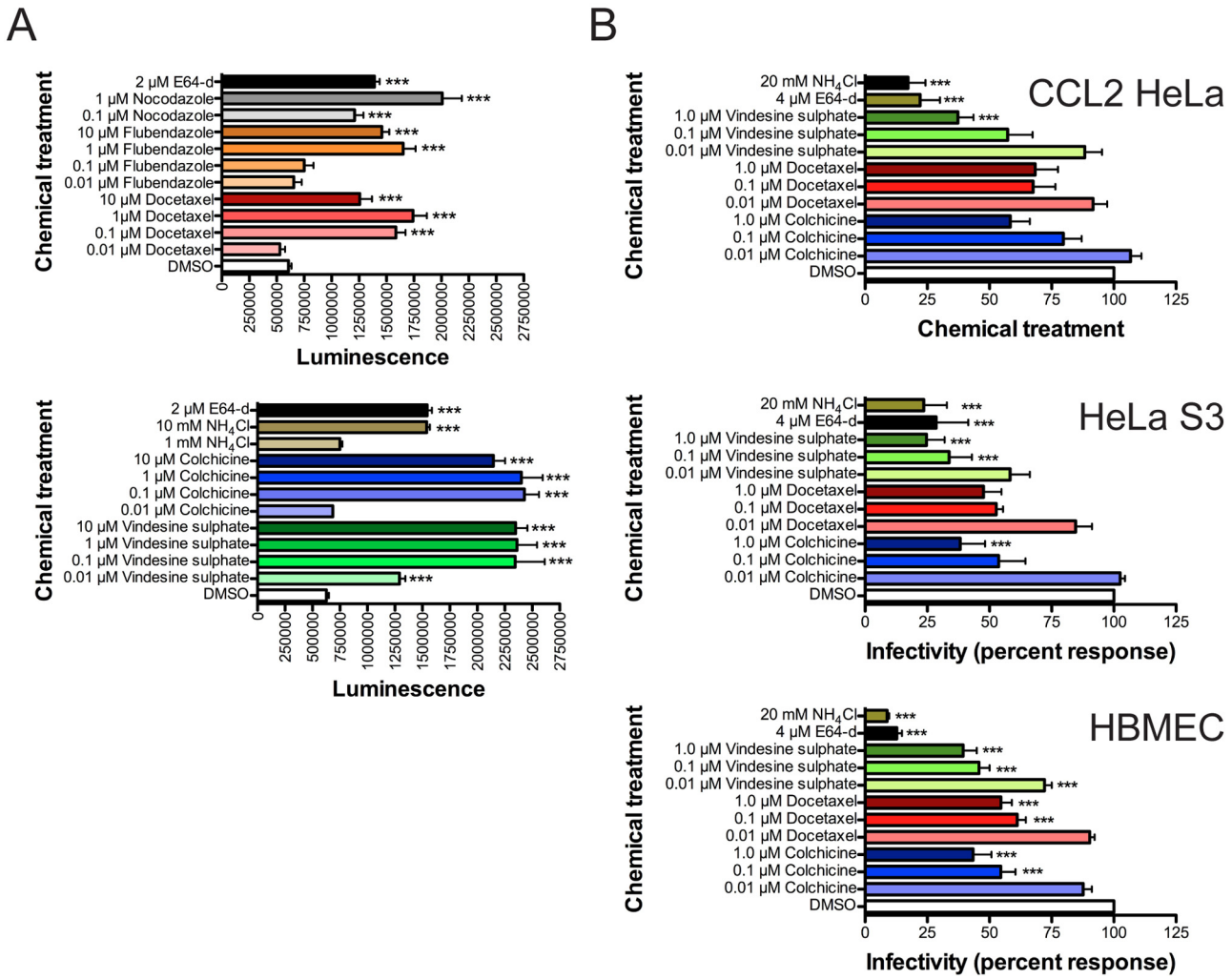

FIG 1 Microtubule-inhibiting compounds diminish reovirus-mediated cytotoxicity and inhibit reovirus infectivity. (A) HeLa S3 cells were incubated with DMSO, increasing concentrations of docetaxel, flubendazole, nocodazole, vindesine sulfate, colchicine, or NH_4Cl, or 2 μM E64-d, adsorbed with T3SA+, and incubated for 48 h. Cell viability was quantified using an ATP-dependent luminescence assay. Results are presented as total luminescence intensity values from experiments performed in quadruplicate. Error bars indicate standard deviations. (B) CCL2 HeLa cells, HeLa S3 cells, or HBMECs were incubated with DMSO or increasing concentrations of colchicine, docetaxel, vindesine sulfate, E64-d, or NH_4Cl and adsorbed with T3SA+ at an MOI of either 5 PFU/cell for HeLa S3 cells and HBMECs or 1 PFU/cell for CCL2 HeLa cells. Cells were incubated in the presence of inhibitors for 20 h and scored for infection by indirect immunofluorescence. Results are presented as percent mean fluorescence intensity compared with DMSO, normalized to cell number and background fluorescence, for quadruplicate experiments with CCL2 HeLa cells and triplicate experiments with HeLa S3 cells and HBMECs. Error bars indicate standard errors of the mean. ***, $P < 0.05$ in comparison to DMSO by one-way ANOVA with Dunnett's multiple-comparison test.

ISVPs, which bind JAM-A at the cell surface but do not require intracellular transport for infection (8, 16–18), CCL2 HeLa cells were treated with DMSO, 20 mM NH_4Cl, or increasing concentrations of vindesine sulfate for 1 h, adsorbed with reovirus virions or ISVPs, and scored for infection by indirect immunofluorescence 20 h after adsorption (Fig. 2B). As observed previously, treatment of cells with NH_4Cl or vindesine sulfate diminished infection following adsorption with virions. In contrast, treatment of cells with NH_4Cl or vindesine sulfate did not significantly alter infection following adsorption with ISVPs. These data indicate that vindesine sulfate blocks a step in reovirus replication following attachment to JAM-A but prior to viral protein synthesis.

Microtubules are required for endocytic sorting of reovirus during cell entry. To determine whether reovirus uses microtubule tracks during cell entry, CCL2 HeLa cells were treated with DMSO or 1 μM vindesine sulfate for 1 h, adsorbed with reovirus, and incubated for 0, 20, or 120 min. Cells were stained for reovirus and α-tubulin and imaged using confocal microscopy (Fig. 3). In DMSO-treated cells, virions were detected on microtubule tracks at 0, 20, and 120 min, with an increasing number of particles observed in the perinuclear area at 120 min. The perinuclear distribution of reovirus virions is consistent with access to late endosomes for disassembly by cathepsin proteases to allow productive infection (13). In vindesine sulfate-treated cells, virions were associated with depolymerized microtubules at 0 and 20 min, but by 120 min, particles appeared to form clusters in the cytoplasm. Treatment of HBMECs with vindesine sulfate also resulted in aggregation of viral particles at 120 min postadsorption, although the clusters were not as prominent as those observed in vindesine

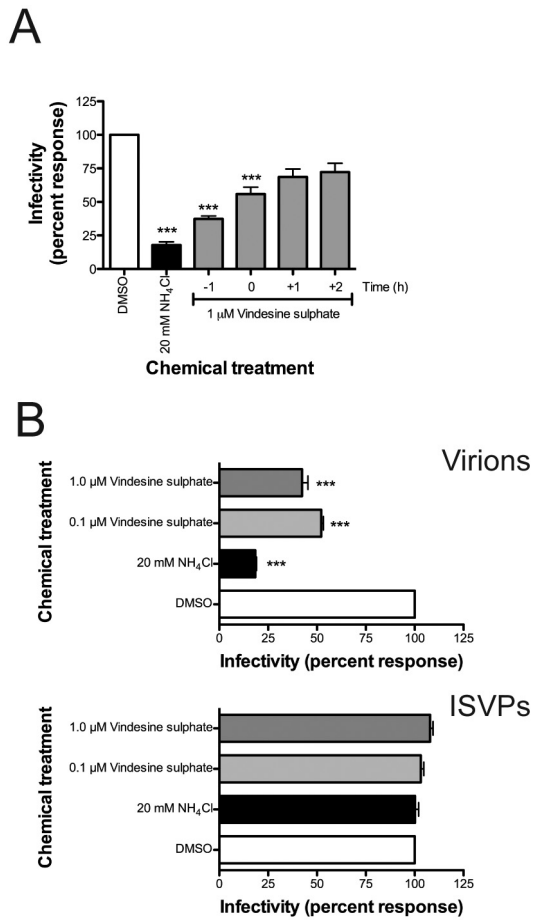

FIG 2 Vindesine sulfate blocks reovirus replication at early times of infection. (A) CCL2 HeLa cells were incubated with DMSO, 20 mM NH_4Cl, or 1 μM vindesine sulfate, adsorbed with T3SA+ at an MOI of 5 PFU/cell, and incubated in the presence of inhibitors for 20 h. Alternatively, cells were incubated with 1 μM vindesine sulfate immediately following adsorption or at 1-h intervals after adsorption. Cells were scored for infection by indirect immunofluorescence. (B) CCL2 HeLa cells were incubated with DMSO, NH_4Cl, or vindesine sulfate, adsorbed with T3SA+ virions or ISVPs at an MOI of 1.63×10^3 particles/cell, and incubated in the presence of inhibitors for 20 h. Cells were scored for infection by indirect immunofluorescence. Results are presented as percent mean fluorescence intensity compared with DMSO, normalized to cell number and background fluorescence, for triplicate experiments. ***, $P < 0.05$ in comparison to DMSO by one-way ANOVA with Dunnett's multiple-comparison test.

sulfate-treated CCL2 HeLa cells (data not shown). These observations suggest that depolymerization of microtubules by vindesine sulfate leads to missorting of reovirus virions during cell entry.

Vindesine sulfate does not affect internalization of reovirus into cells. Since depolymerization of microtubules impairs reovirus intracellular transport and infectivity, we sought to determine whether vindesine sulfate inhibits internalization of viral particles from the cell surface. CCL2 HeLa cells were treated with DMSO or 1 μM vindesine sulfate for 1 h, adsorbed with Alexa 546-labeled reovirus, and incubated for 0, 60, or 120 min. Cells were stained for extracellular virus using reovirus-specific antiserum under nonpermeabilizing conditions, and the ratio of extracellular to internalized reovirus particles was quantified by flow cytometry (Fig. 4A). Over the course of the infection, we observed a decrease in extracellular virus in the presence and absence of vindesine sulfate. These results suggest that vindesine sulfate does not significantly impede internalization of reovirus, at least up to 120 min after adsorption. Consistent with this finding, vindesine sulfate treatment did not diminish cell-surface expression of JAM-A or β1 integrin (data not shown). These results suggest that microtubule function is not required for reovirus attachment or internalization.

Vindesine sulfate impairs reovirus access to intracellular acidified compartments. To determine whether vindesine sulfate alters transport of reovirus to acidified compartments during cell entry, CCL2 HeLa cells were treated with DMSO or 1 μM vindesine sulfate for 1 h, adsorbed with reovirus labeled with a pH-sensitive dye (pHrodo), and incubated for 0, 60, or 120 min. The fluorescence intensity of intracellular virus was quantified by flow cytometry (Fig. 4B). In DMSO-treated cells, mean fluorescence intensity increased over time, indicating that virions gain access to an acidified compartment between 60 and 120 min after adsorption, consistent with prior studies of the kinetics of reovirus delivery to acidified endosomes (13, 30). In contrast, mean fluorescence intensity was dampened during the interval of reovirus entry into vindesine sulfate-treated cells. Importantly, microtubule-inhibiting drugs do not affect the intraluminal pH of endosomes (31). These data suggest that vindesine sulfate impairs reovirus infection by impeding transport of virions to acidified intracellular organelles.

During cell entry, reovirus traverses through Rab5-marked early endosomes en route to Rab7- and Rab9-marked late endosomes for proteolytic disassembly (12). To determine whether vindesine sulfate treatment leads to retention of reovirus particles in early endosomes, CCL2 HeLa cells were transfected with enhanced green fluorescent protein (EGFP)-Rab5A, incubated with DMSO or 1 μM vindesine sulfate for 1 h, adsorbed with Alexa-labeled reovirus, incubated for 120 min, and imaged by confocal microscopy. Analysis of the spectral overlap of fluorescently labeled virions and Rab5A-positive compartments showed no statistically significant difference in the percentages of virions in early endosomes in cells treated with either DMSO or vindesine sulfate (Fig. 4C). These data suggest that inhibition of microtubule function by vindesine sulfate does not lead to an accumulation of reovirus particles in early endosomes.

In a complementary experiment, CCL2 HeLa cells were incubated with DMSO or 1 μM vindesine sulfate for 1 h, adsorbed with Alexa-labeled reovirus, and incubated for 60 or 120 min. Cells were stained for lysosomal-associated membrane protein 1 (LAMP1) to identify late endosomes and lysosomes (Fig. 4D). Analysis of the spectral overlap of fluorescently labeled virions and LAMP1-positive compartments revealed a higher percentage of viral particles distributed to LAMP1-positive endosomes in control-treated cells than in those treated with vindesine sulfate (Fig. 4E). Concordant with these observations, vindesine sulfate decreased reovirus colocalization with Rab7-marked endosomes compared to that seen with control-treated cells (data not shown). Together, these data indicate that although vindesine sulfate does not inhibit reovirus internalization or lead to retention of virus in early endosomes, the drug impedes efficient transport of virions to acidified intracellular compartments where viral disassembly takes place.

Reovirus requires dynein 1 to efficiently infect cells. To determine whether reovirus uses minus-end microtubule motor dy-

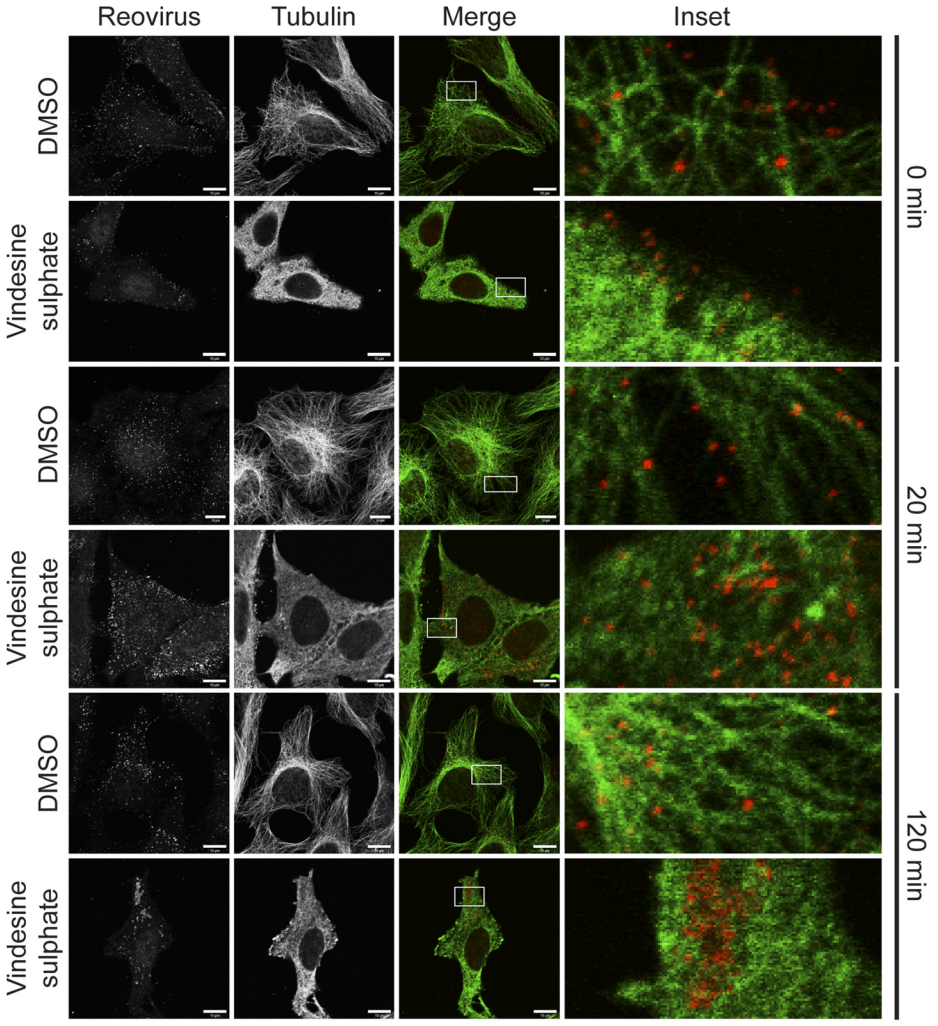

FIG 3 Reovirus uses microtubules to enter cells. CCL2 HeLa cells were adsorbed with T3SA+ at an MOI of 2×10^4 particles/cell at room temperature and incubated at 37°C for 0, 20, or 120 min. Cells were fixed in methanol, stained for reovirus (red) or α-tubulin (green), and imaged by confocal microscopy. Single sections from a Z-stack as well as a merged image are shown for each stain. Insets depict enlarged areas from boxed regions. Scale bars, 10 μm.

nein 1 for transport into the cell interior, HBMECs were transfected with small interfering RNAs (siRNAs) specific for the dynein 1 heavy chain, adsorbed with reovirus strains type 1 Lang (T1L) or type 3 Dearing (T3D), incubated for 48 h, and scored for infection by indirect immunofluorescence (Fig. 5A). Of the cell lines used in this study, diminished expression of dynein 1 caused by RNAi treatment is most efficient in HBMECs (data not shown). Consistent with a requirement for microtubule function for efficient reovirus infection, diminished dynein 1 heavy chain expression caused by RNAi treatment decreased infection by both T1L and T3D. To further define the role of dynein 1 in reovirus cell entry, cells were adsorbed with T1L, incubated for 20 min, stained for reovirus and dynein 1 heavy chain, and imaged by confocal microscopy. Virions were observed in close proximity to dynein 1 in both HBMECs (Fig. 5B) and CCL2 HeLa cells (Fig. 5C), suggesting that reovirus uses dynein 1 to promote cell entry. Together, these data indicate that reovirus requires the microtubule minus-end motor dynein 1 to efficiently infect cells.

CHKV does not require microtubules to infect cells. Chikungunya virus (CHKV), a mosquito-transmitted alphavirus that causes epidemics of arthritis (32), requires acidification to efficiently enter cells, but unlike reovirus, CHKV does not require access to late endosomes (33). To determine whether vindesine sulfate inhibits CHKV infection, BHK-21 cells, which are susceptible to CHKV, were treated with DMSO or 1 μM vindesine sulfate for 1 h, adsorbed with CHKV vaccine strain 181/25 or virulent strain SL15649, incubated for 10 h, and scored for infection by indirect immunofluorescence (Fig. 6A and B). In contrast to findings made in our studies of reovirus, vindesine sulfate did not impair CHKV infection, suggesting that CHKV does not require microtubule function to efficiently enter cells. These results are in agreement with a requirement for microtubules in the maturation of early to late endosomes (34) and provide additional evidence that the drug does not impair reovirus infection by nonspecific cytotoxic effects.

Vindesine sulfate alters reovirus disassembly kinetics. As a final experiment to define the step in reovirus replication blocked by microtubule inhibitors, we tested whether inhibition of microtubule function alters the kinetics of reovirus disassembly. CCL2 HeLa cells were treated with DMSO or 1 μM vindesine sulfate for

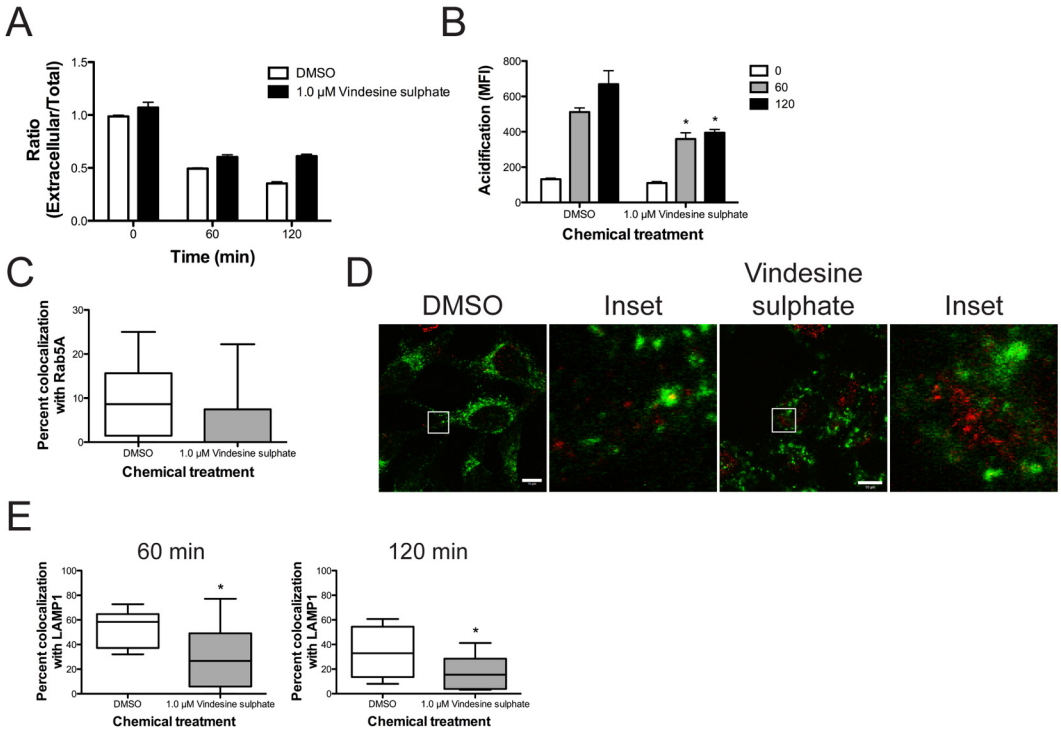

FIG 4 Vindesine sulfate impairs transport of reovirus in the endocytic pathway. (A) CCL2 HeLa cells were incubated with DMSO or 1 μM vindesine sulfate, adsorbed with A546-labeled T3SA+ at an MOI of 5×10^3 particles/cell, and incubated with DMSO or 1 μM vindesine sulfate for the times shown. Cells were stained with reovirus-specific antiserum using nonpermeabilizing conditions. Mean fluorescence intensity (MFI) was assessed by flow cytometry. Results are presented as a ratio of extracellular to total mean fluorescence intensity for triplicate samples. Error bars indicate standard deviations. (B) CCL2 HeLa cells were incubated with DMSO or 1 μM vindesine sulfate, adsorbed with pHrodo-labeled T3SA+ at an MOI of 5×10^3 particles/cell, and incubated with DMSO or 1 μM vindesine sulfate for the times shown. MFI was assessed by flow cytometry. Error bars indicate standard deviations. (C) CCL2 HeLa cells were transfected with EGFP-Rab5A, incubated with DMSO or 1 μM vindesine sulfate, adsorbed with A546-labeled T3SA+ at an MOI of 10^4 particles/cell, and incubated with DMSO or 1 μM vindesine for 120 min. Cells were fixed and imaged by confocal microscopy. Results are expressed as percent colocalization of reovirus particles with Rab5A-positive endosomes ($n = 8$ cells per condition). Error bars indicate minimum and maximum values. (D) CCL2 HeLa cells were incubated with DMSO or 1 μM vindesine sulfate, adsorbed with A546-labeled T3SA+ (red) at an MOI of 10^4 particles/cell, and incubated with DMSO or 1 μM vindesine sulfate for 60 or 120 min. Cells were fixed, stained with a LAMP1-specific antibody (green), and imaged by confocal microscopy. Representative images from 120 min shown. Insets depict enlarged areas of boxed regions. Scale bars, 10 μm. (E) Percent colocalization of reovirus particles with LAMP-1-positive endosomes ($n = 10$ cells per condition). Error bars indicate minimum and maximum values. *, $P < 0.05$ in comparison to DMSO by Student's t test.

1 h, adsorbed with reovirus, and incubated from 0 to 120 min. Whole-cell lysates were resolved by SDS-PAGE and immunoblotted using a reovirus-specific antiserum to detect viral capsid protein μ1 and its major cleavage fragment, δ (Fig. 6C). In control-treated cells, δ was detected by 20 min, with increasing band intensity noted over the experimental time course. In vindesine sulfate-treated cells, δ was not detected until 60 min after adsorption. Densitometric analysis of three independent experiments showed delayed μ1-to-δ conversion at all times tested in vindesine sulfate-treated cells in comparison to control cells (Fig. 6D). We conclude that inhibition of microtubule function leads to inefficient access to acidified endosomal compartments, which in turn delays the disassembly of internalized virions.

DISCUSSION

In this study, we found that reovirus colocalizes with microtubule tracks during cell entry and requires microtubule function and microtubule motor dynein 1 to efficiently traverse the endocytic pathway. Microtubule function is not required for internalization of reovirus virions but rather facilitates targeting of reovirus to acidified endosomes for viral disassembly. Treatment of cells with microtubule inhibitors blocks reovirus infection in a temporal window in which the virus transits from early to late endosomes. These results highlight a new function for microtubules in reovirus replication and suggest that impairment of microtubule activity might diminish infection by viruses that require access to late endosomes to establish productive infection.

Endocytic uptake of macromolecular cargo requires the coordinated action of several host factors, including receptors, Rab GTPases, and enzymes that regulate endocytic transport by modifying targets at specific intracellular sites. For some cargo, microtubules and microtubule-associated motors are required for transport to and from the cell surface. Importantly, the maturation of early to late endosomes is dependent on microtubule function (34). Rab-interacting lysosomal protein (RILP), a Rab7 adapter, recruits dynactin and dynein to late endosomes, promoting late endosome movement toward the cell interior (35). Reovirus is transported to Rab7-marked endosomes during cell entry (13), and expression of dominant-negative RILP inhibits reovirus infection (13). Thus, disruption of microtubule function appears to delay reovirus disassembly by slowing the maturation of the reovirus-containing endosomal fraction. This model is supported by the observed decrease in colocalization of reovirus with LAMP1-marked endosomes. Additional support comes from the

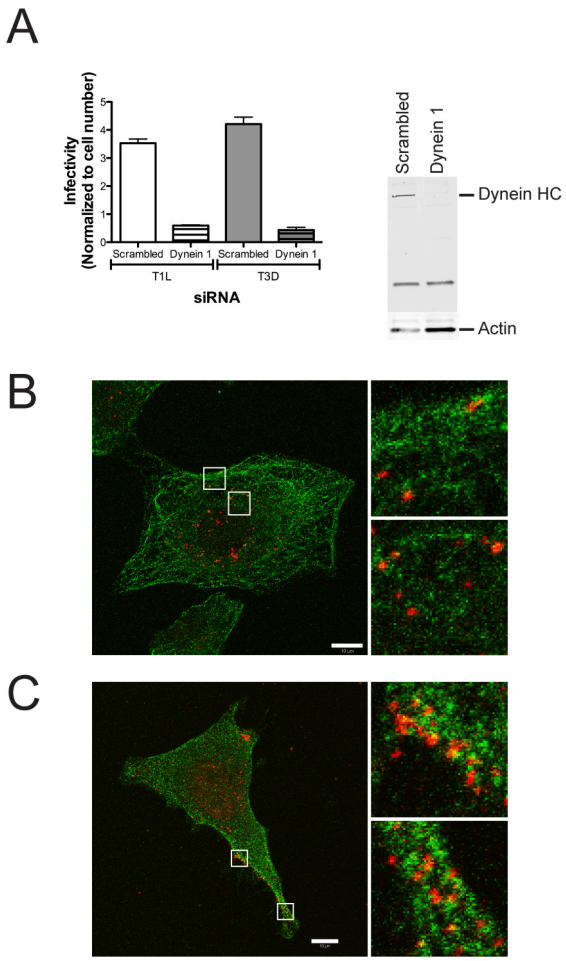

FIG 5 Reovirus uses microtubule motor dynein 1 to efficiently infect cells. (A) (Left panel) HBMECs were transfected with a nonspecific siRNA (scrambled) or an siRNA specific for dynein 1 heavy chain (dynein 1), adsorbed with reovirus strains T1L or T3D at an MOI of 15 PFU/cell, and incubated for 24 h. Cells were scored for infection by indirect immunofluorescence. Results are presented as mean fluorescence intensity normalized to cell number and background fluorescence for triplicate wells. Error bars indicate standard deviations. (Right panel) Whole-cell lysates of HBMECs transfected with nonspecific or dynein 1-specific siRNAs were analyzed by immunoblotting using dynein 1 heavy chain (HC)-specific or actin-specific antibodies. (B and C) HBMECs (B) or CCL2 HeLa cells (C) were adsorbed with T1L at an MOI of 10^4 particles/cell and incubated for 20 min. Cells were stained for reovirus (red) and dynein 1 heavy chain (green) and imaged by confocal microscopy. A single section from a Z-stack is shown. Insets depict enlarged areas from boxed regions. Scale bars, 10 μm.

observation that vindesine sulfate does not diminish infection after adsorption of ISVPs, which are uncoated *in vitro* and thus do not require access to cathepsin-containing organelles to establish infection (16–18). As an important control, vindesine sulfate does not inhibit infection by CHKV, which uncoats in early endosomes (33). Impairment of endosomal maturation might be responsible for the aggregates of reovirus particles observed in vindesine sulfate-treated cells. Interestingly, reovirus virions do not accumulate in early endosomes in cells treated with vindesine sulfate (Fig. 4C). Instead, viral particles in vindesine sulfate-treated cells aggregate in clusters in the cytoplasm. These observations suggest that in the absence of microtubule function, viral particles are missorted during cell entry and not trapped in early endosomes.

Our report highlights the potential for drugs that inhibit endosomal maturation for use as broadly active anti-infectives. Such drugs could inhibit viruses, bacteria, bacterial toxins, and parasites that require access to late endosomes and lysosomes to mediate pathological effects. Avian reovirus, a fusogenic reovirus that, unlike mammalian reovirus, enters cells via caveolin-1 and causes infected cells to form syncytia (36, 37), also uses microtubules to enter cells (36). This finding suggests that employment of microtubules by fusogenic and nonfusogenic reoviruses is a conserved cell entry mechanism despite the use of different endocytic uptake pathways. Adenovirus (38) and Borna disease virus (39) also use microtubules and microtubule motors during cell entry (40). *Enterococcus faecalis* requires microtubules for efficient internalization into cells (41). Cytotoxic necrotizing factor 1 (CNF1), a toxin produced by some pathogenic *Escherichia coli* strains, requires microtubule function to access late endosomes for the processing required for cytotoxicity (42). Flubendazole, a compound identified in our screen as impairing reovirus cytotoxicity, inhibits infection by nematodes (43). While currently available microtubule-inhibiting compounds are associated with significant adverse effects (21), it is possible that safer agents could be developed for anti-infective therapies that transiently inhibit endosomal maturation.

Reovirus strain T3D, which has been trademarked as Reolysin, is being evaluated in clinical trials for efficacy as an oncolytic agent in combination with various chemotherapeutic drugs, including the microtubule inhibitor docetaxel (5). Our findings suggest that pairing reovirus with microtubule-inhibiting agents during oncolytic therapy may limit virus-induced cell killing. Cancer treatment regimens that use reovirus and microtubule-inhibiting drugs may be more efficacious if the administration of virus and chemotherapeutic is not simultaneous. We found that addition of vindesine sulfate to reovirus-infected cells at up to 1 h after infection fails to significantly diminish infection. Thus, we think it important to assess the effects of pharmacological agents on viral infectivity when these treatments are used in combination.

The NCC screen yielded six candidate compounds that do not target microtubules. Procarbazine, which promotes DNA damage (44), and 6-azauridine, which inhibits pyrimidine synthesis (45), likely impair reovirus replication by affecting viral transcription or genome replication. The identification of nicotinic acetylcholine receptor and serotonin receptor agonists as drugs that impair reovirus-induced cytotoxicity points to interesting cellular targets. The nicotinic acetylcholine receptor is expressed in the brain (46), and serotonin receptors are expressed in both the brain and gastrointestinal tract (47). Both of these organs are sites for reovirus replication in the infected host (1). Finally, the identification of indomethacin, which inhibits cyclooxygenase 1 and 2 (48), suggests a yet-uncharacterized function for cyclooxygenases in reovirus replication. Further studies are required to determine whether these drugs inhibit reovirus replication and to define the antiviral mechanisms by which they act.

The identification of host molecules that regulate steps in viral replication enhances an understanding of how viruses use basic cellular processes to propagate and disseminate. These studies also yield new knowledge about cellular functions and illuminate new targets for antiviral drug development. In this study, we used a high-throughput screening approach to identify microtubules and microtubule motor dynein 1 as host factors required for reovirus cell entry, initiation of infection, and consequent cell death.

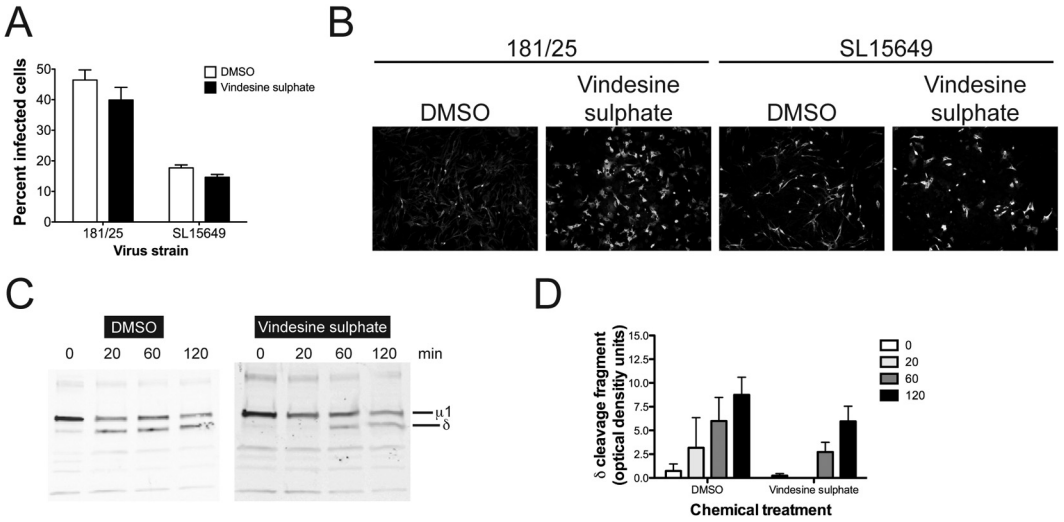

FIG 6 Vindesine sulfate does not affect CHKV infection but alters reovirus disassembly kinetics. (A) BHK-21 cells were incubated with DMSO or 1 μM vindesine sulfate, adsorbed with CHKV strain 181/25 or SL15649 at an MOI of 1 PFU/cell, and incubated with DMSO or vindesine sulfate for 10 h. Cells were stained with CHKV-specific antiserum and DAPI to detect nuclei. Infection was quantified by indirect immunofluorescence. Results are presented as percent infected cells from triplicate wells. Error bars indicate standard deviations. (B) Images of DMSO- or vindesine sulfate-treated BHK-21 cells infected with CHKV strain 181/25 or SL15659 and stained with CHKV-specific antiserum. (C) CCL2 HeLa cells were incubated with DMSO or 1 μM vindesine sulfate, adsorbed with T3SA+ at an MOI of 10 PFU/cell, and incubated with DMSO or 1 μM vindesine sulfate for the times shown. Whole-cell lysates were immunoblotted using reovirus-specific antiserum. (D) Densitometric analysis of the δ cleavage fragment of reovirus μ1 protein from triplicate experiments. Error bars indicate standard errors of the mean. The key indicates times in minutes.

Findings made in this study should contribute to the development of improved strategies for use of reovirus as an oncolytic and establish a platform for testing microtubule inhibitors as antiinfective agents.

MATERIALS AND METHODS

Cells, viruses, chemical inhibitors, and antibodies. Spinner-adapted murine L929 cells, CCL2 HeLa cells, HeLa S3 cells, and HBMECs were cultivated as previously described (13, 28). BHK-21 and Vero81 cells were cultivated in Alpha minimal essential medium (MEM) (Sigma) supplemented to contain 5% fetal bovine serum (FBS) (Vero81) or 10% FBS (BHK-21) and L-glutamine. Medium for all cells was supplemented with penicillin-streptomycin (Invitrogen) and amphotericin B (Sigma).

Purified virions of reovirus strains T1L, T3D, and T3SA+ were prepared by plaque purification and passage using L929 cells as previously described (12, 13, 28). ISVPs were generated by treating particles with α-chymotrypsin (Sigma) as previously described (12). Reovirus virions were labeled with succinimidyl ester Alexa Fluor 546 (A546) or pHrodo SE (pHrodo) (Invitrogen) as previously described (13).

CHKV strain 181/25 was provided by Robert Tesh (University of Texas Medical Branch). Viral RNA was isolated from a plaque-purified isolate, and cDNA was generated using random hexamers. Overlapping fragments were amplified, cloned into pCR2.1 TOPO (Invitrogen), and sequenced. The 5′ untranslated region was sequenced using 5′ rapid amplification of cDNA ends. An infectious clone was synthesized by GenScript (Piscataway, NJ) in four fragments. Genome fragments were assembled and subcloned into pSinRep5 low-copy-number plasmid. The CHKV strain SL15649 infectious clone was provided by Mark Heise (University of North Carolina at Chapel Hill) (49). Infectious clone plasmids for 181/25 and SL15649 were linearized and transcribed *in vitro* using an mMessage mMachine SP6 transcription kit (Ambion). BHK-21 cells were electroporated with viral RNA and incubated at 37°C for 24 h. Supernatants containing progeny virus were harvested from electroporated cells and stored at −80°C. All experiments using SL15649 were performed using biosafety level 3 conditions.

Ammonium chloride (NH_4Cl; Gibco) was resuspended in water. E64-d, colchicine, nocodazole (Sigma), docetaxel, flubendazole, and vindesine sulfate (Sequoia Research Products) were resuspended in DMSO. The immunoglobulin G (IgG) fraction of a rabbit antiserum raised against T1L or T3D was purified as previously described (6). LAMP1-specific and dynein heavy chain-specific monoclonal antibodies (Abcam), α-tubulin-specific monoclonal antibody (Cell Signaling Technology), actin-specific polyclonal antiserum (Santa Cruz Biotechnology), and CHKV-specific antiserum (ATCC) were used for indirect immunofluorescence experiments, infectivity assays, and immunoblot analyses. Alexa Fluor-conjugated antibodies (Invitrogen) were used as secondary antibodies.

Cell viability assay. HeLa S3 cells were incubated with OMEM-1 (Invitrogen) medium containing DMSO, E64-d, NH_4Cl, or microtubule inhibitors at 37°C for 1 h and adsorbed with T3SA+ at a multiplicity of infection (MOI) of 200 PFU/cell in the presence of DMSO, E64-d, NH_4Cl, or microtubule inhibitors in OMEM-I medium at 37°C for 48 h. Cell viability was quantified using the Cell Titer Glo assay.

Quantification of reovirus infectivity. Reovirus infectivity was assessed by indirect immunofluorescence (50). Cells were incubated with complete medium containing DMSO or chemical inhibitors at 37°C for 1 h, adsorbed with reovirus at room temperature for 1 h, and incubated with complete medium containing DMSO or chemical inhibitors at 37°C for 20 h. Cells were fixed and stained with reovirus-specific antiserum and goat anti-rabbit IRDye 800 (Li-COR), DRAQ5 (Cell Signaling), and Sapphire700 (Li-COR). Immunofluorescence was detected using a Li-COR Odyssey infrared imaging system (Li-COR). Infectivity was quantified using the In-Cell Western feature of the Odyssey software suite.

Confocal microscopy of reovirus-infected cells. Confocal microscopy of reovirus-infected cells was performed as previously described (12, 13). HeLa CCL2 cells were incubated with complete medium containing DMSO or vindesine sulfate at 37°C for 1 h. Cells were adsorbed with reovirus at an MOI of 2×10^4 particles/cell and either fixed with ice-cold methanol or incubated in complete medium containing DMSO or vindesine sulfate at 37°C for 120 min followed by fixation with ice-cold methanol. Cells were incubated with reovirus-specific polyclonal and α-tubulin-specific antiserum followed by Alexa Fluor IgG A488 or A546.

Coverslips were placed on slides using aqua-Poly/Mount mounting medium (Polysciences, Inc.).

Colocalization of reovirus particles with Rab5A-positive endosomes was assessed by transfecting CCL2 HeLa cells with EGFP-Rab5A (13) using Fugene 6 (Roche). Cells were incubated at 37°C for 24 h, incubated with medium containing DMSO or vindesine sulfate at 37°C for 1 h, adsorbed with A546-labeled reovirus at an MOI of 10^4 particles/cell, incubated with complete medium containing DMSO or vindesine sulfate for 120 min, fixed for 20 min with 10% formalin, quenched with 0.1 M glycine, washed with phosphate-buffered saline (PBS), and placed on slides using aqua-Poly/Mount mounting medium.

Colocalization of reovirus particles with LAMP1-positive endosomes was determined by incubating CCL2 HeLa cells with complete medium containing DMSO or vindesine sulfate at 37°C for 1 h followed by adsorption with A546-labeled reovirus at an MOI of 10^4 particles/cell and incubation with complete medium containing DMSO or vindesine sulfate for various intervals, after which the cells were fixed and stained with LAMP1-specific antibody. Colocalization of reovirus particles with dynein 1 was determined by adsorbing HBMECs or CCL2 HeLa cells with reovirus at an MOI of 10^4 particles/cell, after which the cells were incubated with complete medium for 20 min, fixed in methanol, and stained with reovirus-specific antiserum and dynein heavy chain-specific antibody.

Images were captured using a Zeiss LSM 510 Meta laser scanning confocal microscope and a 63×/1.40 numerical aperture (NA) Plan-Apochromat oil objective. Pinhole sizes were identical for all fluors. Images were normalized for pixel intensity, brightness, and contrast. Single sections of 0.39 μM thickness from a Z-stack are presented. Colocalization was determined using the Profile function of LSM Image software (Zeiss) (12, 13).

Flow cytometric analysis of reovirus internalization. CCL2 HeLa cells were treated with DMSO or vindesine sulfate in complete medium at 37°C for 1 h and adsorbed with A546-labeled reovirus at an MOI of 5×10^3 particles/cell at room temperature for 1 h. The inoculum was removed, and cells were incubated with complete medium containing DMSO or vindesine sulfate for various intervals. Cells were detached with Cellstripper (Cellgro) at 37°C for 15 min, quenched with fluorescence-activated cell sorter (FACS) buffer (PBS with 2% FBS), and stained with reovirus-specific polyclonal antiserum in FACS buffer at 4°C for 30 min. Cells were washed with FACS buffer, stained with Alexa Fluor-conjugated antibodies in FACS buffer at 4°C for 30 min, and fixed in PBS with 1% electron microscopy (EM)-grade paraformaldehyde (FACS Fix; Electron Microscopy Sciences).

Flow cytometric analysis of reovirus acidification was performed as previously described (13). Cells were treated with DMSO or vindesine sulfate in complete medium at 37°C for 1 h, adsorbed with pHrodo-labeled reovirus at an MOI of 5×10^3 particles/cell, incubated in complete medium containing DMSO or vindesine sulfate for various intervals, and fixed in FACS Fix. Cell staining was assessed using a BD LSRII flow cytometer and quantified using FlowJo software.

Knockdown of dynein 1 heavy chain by RNAi. HBMECs were transfected with 10 nM nonspecific siRNA or an siRNA specific for the dynein 1 heavy chain using Lipofectamine RNAi Max (Invitrogen) according to the manufacturer's instructions. Cells were incubated at 37°C for 48 h, adsorbed with reovirus at an MOI of 15 PFU/cell at room temperature for 1 h, and incubated at 37°C for 24 h. Cells were fixed with methanol and scored for infection by indirect immunofluorescence.

Immunoblotting for dynein 1 heavy chain. Immunoblot analysis of cell lysates was performed as previously described (12). Total cell lysates of HBMECs transfected with nonspecific or dynein 1 heavy chain-specific siRNAs were resolved by SDS-PAGE and immunoblotted with primary antibodies specific for dynein 1 heavy chain and actin. Membranes were scanned using an Odyssey imaging system, and band intensity was quantified using the Odyssey software suite.

CHKV infectivity assay. BHK-21 cells were incubated with DMSO or vindesine sulfate in complete medium at 37°C for 1 h and adsorbed with CHKV strain 181/25 or SL15649 at an MOI of 1 PFU/cell in the presence of DMSO or vindesine sulfate at 37°C for 1 h. The inoculum was removed, and cells were incubated with complete medium containing DMSO or vindesine sulfate at 37°C for 10 h. Cells were fixed with ice-cold methanol and incubated with CHKV-specific polyclonal antiserum, A488-labeled IgG, and 4′,6-diamidino-2-phenylindole (DAPI; Invitrogen). Cells were visualized using an Axiovert 200 fluorescence microscope (Zeiss). CHKV-positive cells were enumerated in three fields of view for triplicate samples and normalized to total cells per field.

Assessment of reovirus disassembly kinetics. CCL2 HeLa cells were treated with DMSO or vindesine sulfate in complete medium at 37°C for 1 h, adsorbed with reovirus at an MOI of 10 PFU/cell at room temperature for 1 h, and incubated in complete medium with DMSO or vindesine sulfate for various intervals. Total cell lysates were resolved by SDS-PAGE and immunoblotted with reovirus-specific polyclonal antiserum. Immunoblots were quantified by densitometry analysis using Odyssey software.

Statistical analysis. Mean values for at least triplicate experiments were compared using one-way analysis of variance (ANOVA) with Dunnett's multiple-comparison test (Graph Pad Prism). P values of <0.05 were considered to be statistically significant. Alternatively, samples were compared using an unpaired Student's t test (Graph Pad Prism). P values of <0.05 were considered to be statistically significant.

SUPPLEMENTAL MATERIAL

Supplemental material for this article may be found at http://mbio.asm.org/lookup/suppl/doi:10.1128/mBio.00405-13/-/DCSupplemental.

Text S1, DOCX file, 0.1 MB.
Figure S1, TIF file, 8.9 MB.
Table S1, PDF file, 0.1 MB.

ACKNOWLEDGMENTS

We thank Jennifer Konopka and Caroline Lai for critical review of the manuscript. We are grateful to members of the Dermody laboratory for useful suggestions during the course of this study. Small-molecule screening was conducted with assistance from the Vanderbilt High-Throughput Screening Facility. Confocal microscopy experiments were conducted in the Vanderbilt Cell Imaging Shared Resource. Flow cytometry experiments were performed in the Vanderbilt Cytometry Shared Resource.

This work was supported by Public Health Service awards T32 HL07751 (B.A.M. and A.W.A.), F32 A1801082 (B.A.M.), R01 AI32539 (T.S.D.), and U54 AI057157 (T.S.D.) and by the Elizabeth B. Lamb Center for Pediatric Research. Additional support was provided by Public Health Service awards P30 CA68485 for the Vanderbilt-Ingram Cancer Center and P60 DK20593 for the Vanderbilt Diabetes Research and Training Center.

REFERENCES

1. **Dermody TS, Parker J, Sherry B.** 2013. Orthoreoviruses. pp. 1304–1346. *In* Knipe DM, Howley PM (ed.), Fields virology, vol. 2, 6th ed., Lippincott Williams & Wilkins, Philadelphia, PA.
2. **Ouattara LA, Barin F, Barthez MA, Bonnaud B, Roingeard P, Goudeau A, Castelnau P, Vernet G, Paranhos-Baccalà G, Komurian-Pradel F.** 2011. Novel human reovirus isolated from children with acute necrotizing encephalopathy. Emerg. Infect. Dis. **17:**1436–1444.
3. **Kobayashi T, Antar AA, Boehme KW, Danthi P, Eby EA, Guglielmi KM, Holm GH, Johnson EM, Maginnis MS, Naik S, Skelton WB, Wetzel JD, Wilson GJ, Chappell JD, Dermody TS.** 2007. A plasmid-based reverse genetics system for animal double-stranded RNA viruses. Cell Host Microbe **1:**147–157.
4. **London SD, Cebra-Thomas JA, Rubin DH, Cebra JJ.** 1990. CD8 lymphocyte subpopulations in Peyer's patches induced by reovirus serotype 1 infection. J. Immunol. **144:**3187–3194.
5. **Maitra R, Ghalib MH, Goel S.** 2012. Reovirus: a targeted therapeutic—progress and potential. Mol. Cancer Res. **10:**1514–1525.
6. **Barton ES, Connolly JL, Forrest JC, Chappell JD, Dermody TS.** 2001.

Utilization of sialic acid as a coreceptor enhances reovirus attachment by multistep adhesion strengthening. J. Biol. Chem. **276:**2200–2211.
7. **Reiss K, Stencel JE, Liu Y, Blaum BS, Reiter DM, Feizi T, Dermody TS, Stehle T.** 2012. The GM2 glycan serves as a functional coreceptor for serotype 1 reovirus. PLoS Pathog. **8:**e1003078. doi: 10.1371/journal.ppat.1003078.
8. **Barton ES, Forrest JC, Connolly JL, Chappell JD, Liu Y, Schnell FJ, Nusrat A, Parkos CA, Dermody TS.** 2001. Junction adhesion molecule is a receptor for reovirus. Cell **104:**441–451.
9. **Campbell JA, Schelling P, Wetzel JD, Johnson EM, Wilson GA, Forrest JC, Aurrand-Lions M, Imhof BA, Stehle T, Dermody TS.** 2005. Junctional adhesion molecule-A serves as a receptor for prototype and field-isolate strains of mammalian reovirus. J. Virol. **79:**7967–7978.
10. **Forrest JC, Campbell JA, Schelling P, Stehle T, Dermody TS.** 2003. Structure-function analysis of reovirus binding to junctional adhesion molecule 1. Implications for the mechanism of reovirus attachment. J. Biol. Chem. **278:**48434–48444.
11. **Maginnis MS, Forrest JC, Kopecky-Bromberg SA, Dickeson SK, Santoro SA, Zutter MM, Nemerow GR, Bergelson JM, Dermody TS.** 2006. Beta1 integrin mediates internalization of mammalian reovirus. J. Virol. **80:**2760–2770.
12. **Mainou BA, Dermody TS.** 2011. Src kinase mediates productive endocytic sorting of reovirus during cell entry. J. Virol. **85:**3203–3213.
13. **Mainou BA, Dermody TS.** 2012. Transport to late endosomes is required for efficient reovirus infection. J. Virol. **86:**8346–8358.
14. **Ebert DH, Deussing J, Peters C, Dermody TS.** 2002. Cathepsin L and cathepsin B mediate reovirus disassembly in murine fibroblast cells. J. Biol. Chem. **277:**24609–24617.
15. **Maratos-Flier E, Goodman MJ, Murray AH, Kahn CR.** 1986. Ammonium inhibits processing and cytotoxicity of reovirus, a nonenveloped virus. J. Clin. Invest. **78:**1003–1007.
16. **Sturzenbecker LJ, Nibert M, Furlong D, Fields BN.** 1987. Intracellular digestion of reovirus particles requires a low pH and is an essential step in the viral infectious cycle. J. Virol. **61:**2351–2361.
17. **Borsa J, Morash BD, Sargent MD, Copps TP, Lievaart PA, Szekely JG.** 1979. Two modes of entry of reovirus particles into L cells. J. Gen. Virol. **45:**161–170.
18. **Boulant S, Stanifer M, Kural C, Cureton DK, Massol R, Nibert ML, Kirchhausen T.** 2013. Similar uptake but different trafficking and escape routes of reovirus virions and ISVPs imaged in polarized MDCK cells. Mol. Biol. Cell, **24:**1196–1207.
19. **Jordan MA.** 2002. Mechanism of action of antitumor drugs that interact with microtubules and tubulin. Curr. Med. Chem. Anticancer Agents **2:**1–17.
20. **Dumontet C, Jordan MA.** 2010. Microtubule-binding agents: a dynamic field of cancer therapeutics. Nat. Rev. Drug Discov. **9:**790–803.
21. **McGrogan BT, Gilmartin B, Carney DN, McCann A.** 2008. Taxanes, microtubules and chemoresistant breast cancer. Biochim. Biophys. Acta **1785:**96–132.
22. **Guéritte F.** 2001. General and recent aspects of the chemistry and structure-activity relationships of taxoids. Curr. Pharm. Des. **7:**1229–1249.
23. **Duflos A, Kruczynski A, Barret JM.** 2002. Novel aspects of natural and modified vinca alkaloids. Curr. Med. Chem. Anticancer Agents **2:**55–70.
24. **Gennerich A, Vale RD.** 2009. Walking the walk: how kinesin and dynein coordinate their steps. Curr. Opin. Cell Biol. **21:**59–67.
25. **Danthi P, Coffey CM, Parker JS, Abel TW, Dermody TS.** 2008. Independent regulation of reovirus membrane penetration and apoptosis by the mu1 phi domain. PLoS Pathog. **4:**e1000248. doi:10.1371/journal.ppat.1000248.
26. **Ebert DH, Wetzel JD, Brumbaugh DE, Chance SR, Stobie LE, Baer GS, Dermody TS.** 2001. Adaptation of reovirus to growth in the presence of protease inhibitor E64 segregates with a mutation in the carboxy terminus of viral outer-capsid protein sigma3. J. Virol. **75:**3197–3206.
27. **Connolly JL, Barton ES, Dermody TS.** 2001. Reovirus binding to cell surface sialic acid potentiates virus-induced apoptosis. J. Virol. **75:**4029–4039.
28. **Lai CM, Mainou BA, Kim KS, Dermody TS.** 2013. Directional release of reovirus from the apical surface of polarized endothelial cells. mBio **4:**e00049-13. doi: 10.1128/mBio.00049-13.
29. **Weatherbee JA, Luftig RB, Weihing RR.** 1978. In vitro polymerization of microtubules from HeLa cells. J. Cell Biol. **78:**47–57.
30. **Doyle JD, Danthi P, Kendall EA, Ooms LS, Wetzel JD, Dermody TS.** 2012. Molecular determinants of proteolytic disassembly of the reovirus outer capsid. J. Biol. Chem. **287:**8029–8038.
31. **Bayer N, Schober D, Prchl E, Murphy RF, Blaas D, Fuchs R.** 1998. Effect of bafilomycin A1 and nocodazole on endocytic transport in HeLa cells: implications for viral uncoating and infection. J. Virol. **72:**9645–9655.
32. **Pastorino B, Muyembe-Tamfum JJ, Bessaud M, Tock F, Tolou H, Durand JP, Peyrefitte CN.** 2004. Epidemic resurgence of chikungunya virus in democratic Republic of the Congo: identification of a new Central African strain. J. Med. Virol. **74:**277–282.
33. **Bernard E, Solignat M, Gay B, Chazal N, Higgs S, Devaux C, Briant L.** 2010. Endocytosis of chikungunya virus into mammalian cells: role of clathrin and early endosomal compartments. PLoS One **5:**e11479. doi: 10.1371/journal.pone.0011479.
34. **Huotari J, Helenius A.** 2011. Endosome maturation. EMBO J. **30:**3481–3500.
35. **Jordens I, Fernandez-Borja M, Marsman M, Dusseljee S, Janssen L, Calafat J, Janssen H, Wubbolts R, Neefjes J.** 2001. The Rab7 effector protein RILP controls lysosomal transport by inducing the recruitment of dynein-dynactin motors. Curr. Biol. **11:**1680–1685.
36. **Huang WR, Wang YC, Chi PI, Wang L, Wang CY, Lin CH, Liu HJ.** 2011. Cell entry of avian reovirus follows a caveolin-1-mediated and dynamin-2-dependent endocytic pathway that requires activation of p38 mitogen-activated protein kinase (MAPK) and Src signaling pathways as well as microtubules and small GTPase Rab5 protein. J. Biol. Chem. **286:**30780–30794.
37. **Salsman J, Top D, Boutilier J, Duncan R.** 2005. Extensive syncytium formation mediated by the reovirus FAST proteins triggers apoptosis-induced membrane instability. J. Virol. **79:**8090–8100.
38. **Bremner KH, Scherer J, Yi J, Vershinin M, Gross SP, Vallee RB.** 2009. Adenovirus transport via direct interaction of cytoplasmic dynein with the viral capsid hexon subunit. Cell Host Microbe **6:**523–535.
39. **Clemente R, de la Torre JC.** 2009. Cell entry of Borna disease virus follows a clathrin-mediated endocytosis pathway that requires Rab5 and microtubules. J. Virol. **83:**10406–10416.
40. **Hsieh MJ, White PJ, Pouton CW.** 2010. Interaction of viruses with host cell molecular motors. Curr. Opin. Biotechnol. **21:**633–639.
41. **Millán D, Chiriboga C, Patarroyo MA, Fontanilla MR.** 2013. Enterococcus faecalis internalization in human umbilical vein endothelial cells (HUVEC). Microb. Pathog. **57:**62–69.
42. **Contamin S, Galmiche A, Doye A, Flatau G, Benmerah A, Boquet P.** 2000. The p21 Rho-activating toxin cytotoxic necrotizing factor 1 is endocytosed by a clathrin-independent mechanism and enters the cytosol by an acidic-dependent membrane translocation step. Mol. Biol. Cell **11:**1775–1787.
43. **Hanser E, Mehlhorn H, Hoeben D, Vlaminck K.** 2003. In vitro studies on the effects of flubendazole against Toxocara canus and Ascaris suum. Parasitol. Res. **89:**63–74.
44. **Erikson JM, Tweedie DJ, Ducore JM, Prough RA.** 1989. Cytotoxicity and DNA damage caused by the azoxy metabolites of procarbazine in L1210 tumor cells. Cancer Res. **49:**127–133.
45. **Tatibana M, Kita K, Asai T.** 1982. Stimulation by 6-azauridine of carbamoyl phosphate synthesis for pyrimidine biosynthesis in mouse spleen slices. Eur. J. Biochem. **128:**625–629.
46. **Changeux JP.** 2012. The nicotinic acetylcholine receptor: the founding father of the pentameric ligand-gated ion channel superfamily. J. Biol. Chem. **287:**40207–40215.
47. **Hannon J, Hoyer D.** 2008. Molecular biology of 5-HT receptors. Behav. Brain Res. **195:**198–213.
48. **Dannhardt G, Kiefer W.** 2001. Cyclooxygenase inhibitors—current status and future prospects. Eur. J. Med. Chem. **36:**109–126.
49. **Morrison TE, Oko L, Montgomery SA, Whitmore AC, Lotstein AR, Gunn BM, Elmore SA, Heise MT.** 2011. A mouse model of chikungunya virus-induced musculoskeletal inflammatory disease: evidence of arthritis, tenosynovitis, myositis, and persistence. Am. J. Pathol. **178:**32–40.
50. **Iskarpatyoti JA, Willis JZ, Guan J, Morse EA, Ikizler M, Wetzel JD, Dermody TS, Contractor N.** 2012. A rapid, automated approach for quantitation of rotavirus and reovirus infectivity. J. Virol. Methods **184:**1–7.